Journal of The Electrochemical Society, **156** (10) H767-H771 (2009)
0013-4651/2009/156(10)/H767/5/$25.00 © The Electrochemical Society

Photoelectrochemical Undercut Etching of *m*-Plane GaN for Microdisk Applications

Adele C. Tamboli,[z] Mathew C. Schmidt, Asako Hirai, Steven P. DenBaars, and Evelyn L. Hu

Materials Department, University of California, Santa Barbara, California 93106-5050, USA

Undercut etching is a necessary technique for a variety of device applications, including microdisk lasers. We have explored bandgap-selective photoelectrochemical etching of nonpolar *m*-plane GaN for undercut etching applications, including microdisks. These nonpolar optical devices are not limited by the quantum-confined Stark effect that hampers the performance of polar *c*-plane GaN devices. We discuss the dependence of undercut quality on etchant concentration, illumination intensity, masking material, and epitaxial structure and use this technique to fabricate *m*-plane microdisks. In these nonpolar microdisks, the in-plane polarization fields have a dramatic effect on the symmetry of the etching in both the undercut etching and in the unwanted etching of the GaN disk layer. With a careful balance of etchant concentration and illumination intensity and a well-designed epitaxial structure, we have achieved smoother optical cavities than were possible in *c*-plane GaN.
 [DOI: 10.1149/1.3184156]

Manuscript submitted April 6, 2009; revised manuscript received June 26, 2009. Published August 3, 2009.

Nonpolar *m*-plane GaN has received significant interest for optical devices recently because it lacks the strong polarization fields along the growth direction that hamper the performance of more easily grown *c*-plane GaN.[1,2] Recently, GaN substrates have become available in many different crystallographic orientations, enabling the growth of III-nitride devices along nonpolar and semipolar directions with low defect densities. These nonpolar planes do not suffer from the quantum-confined Stark effect, which reduces the efficiency of *c*-oriented quantum wells by spatially separating the electron and hole wave functions. We have recently reported on top-down photoelectrochemical (PEC) etching of *m*-plane GaN for a variety of device applications.[3] PEC etching is a photoassisted wet etch technique that allows ion-damage free etching of GaN and its alloys at room temperature. This technique is particularly promising for *m*-plane devices because the lower defect density and reduced chemical stability of the *m*-plane facet, compared to the Ga face exposed after *c*-plane growth, allow for much smoother and more controllable etching in *m*-plane devices. Undercut etching is desirable for a variety of device applications, including photonic crystal membranes,[4] microelectromechanical systems,[5] air-gap distributed Bragg reflectors,[6] and microdisks.[7] PEC etching is one of only a few techniques that can be used for undercut etching of GaN.[8] In this paper, we discuss PEC undercut etching of *m*-plane GaN, focusing on microdisk laser applications as a sample system.

To highlight our discussions on the characterization of the etch process, we focus on the challenges surrounding the undercut etching of *m*-plane microdisks. Microdisks consist of a circular resonant cavity, where light propagates along the periphery of the disk, confined to whispering gallery modes. In the vertical direction, light is confined to a single mode thickness cavity by the index contrast between the semiconducting disk and the surrounding air. The disk, which is supported in the center by a post that does not overlap with the modes, must be fully and smoothly undercut by a selective wet etch to achieve optical isolation with minimal scattering losses. For this process, we use bandgap-selective PEC etching to selectively remove a lower bandgap sacrificial InGaN layer. Bandgap-selective PEC etching has been used for undercut etching of many *c*-plane GaN devices previously,[5,6,9-11] and we have reported on *c*-plane GaN microdisks fabricated using this method that had a record-low lasing threshold under room temperature and continuous-wave operation.[7] Microdisks fabricated in *m*-plane GaN have the potential for an even better performance because they are not limited by the quantum-confined Stark effect. This paper discusses the optimization of the PEC etch process, focusing on *m*-plane microdisk structures as an example. An optimized PEC undercut etching process can have broad application to a variety of *m*-plane devices.

Experimental

Samples were grown by metallorganic chemical vapor deposition on *m*-plane GaN substrates provided by Mitsubishi Chemical Corporation. The epitaxial structure varied in complexity from simple passive cavity microdisks, which consisted of 120 nm unintentionally doped GaN on top of a 200 nm InGaN post, to a full microdisk structure with quantum wells and pin doping. In all cases, samples were coated in 50 nm SiO_2 as a hard mask, and then circles ranging from 6 to 12 μm were defined by optical lithography. Mesas were etched using a CHF_3 reactive ion etch to transfer the pattern into SiO_2 and then a Cl_2 reactive ion etch to dry etch GaN mesas through the post and into the underlying GaN template. In most cases, the SiO_2 hard mask was then removed in buffered HF. Concentric circles were masked off, covering these mesas, and a Ti/Pt 50/300 Å bilayer was deposited in the field around the mesas as a cathode for PEC etching. PEC undercut etching was performed in HCl of varying concentrations at room temperature and with no applied bias. The illumination source was either a 1000 W broad-band Xe lamp filtered through a GaN wafer to excite only the InGaN layers or a 25 W light-emitting diode (LED) array with a center wavelength of 405 nm. Samples were examined using a scanning electron microscope (SEM).

Results and Discussion

Passive cavities.— While a fully functional microdisk structure includes a variety of different layers, including quantum wells, cladding layers, and doping, it is instructive to first study the undercut etching behavior of a very simple epitaxial structure. In this case, we used a 120 nm thick GaN layer on top of a 200 nm thick $In_{0.05}Ga_{0.95}N$ sacrificial layer, grown on an n-type GaN template and substrate. For these experiments, we performed PEC etching using a 1000 W Xe lamp with a GaN filter to selectively excite carriers in the InGaN layer only, and samples were immersed in HCl of varying concentrations. The electron–hole pairs were generated in the InGaN, and electrons were extracted into a solution by the cathode, while the holes traveled to the InGaN surface and participated in oxidation reactions. This oxide was dissolved in the HCl, resulting in etching.[12] The interplay of hole confinement, chemical reactivity, and electrolyte strength gives rise to a variety of different etched profiles. This situation is illustrated schematically in Fig. 1, where (a) shows a diagram of hole generation and consumption in these passive cavity structures, leading to etching in various different areas and (b) is a schematic energy band diagram of a GaN/InGaN/GaN structure where the top GaN surface is in contact with an electrolyte. The electron–hole pairs were generated in the InGaN

[z] E-mail: atamboli@umail.ucsb.edu

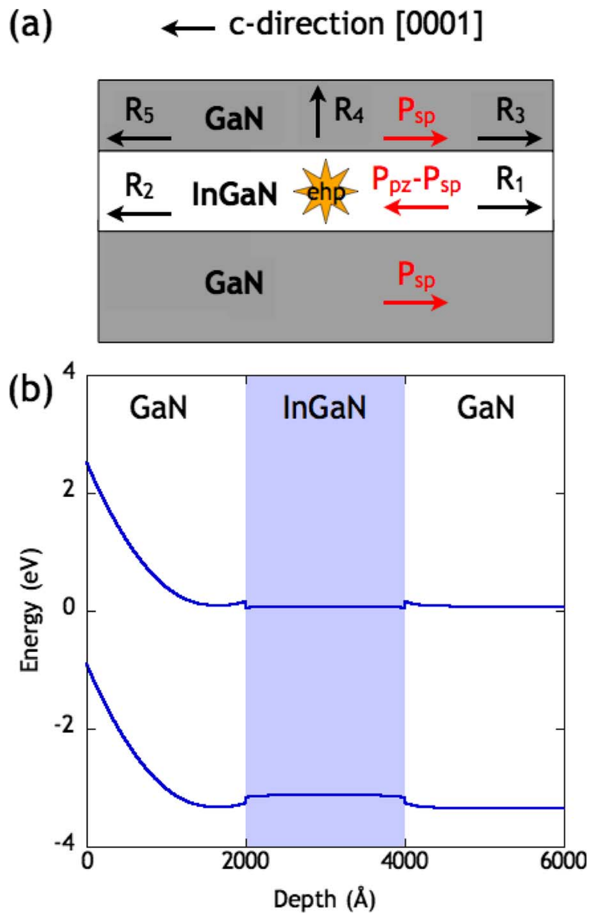

Figure 1. (Color online) (a) Diagram of etch rates for various parts of these structures: The undercut etch rates, R_1 and R_2, depend on the hole generation rate and the etchant concentration (rate of hole consumption). The etch rates for the GaN disk, R_3, R_4, and R_5, become comparable to R_1 and R_2 only when the electrolyte is dilute, such that the consumption of holes is slow enough that some diffuse into the GaN disk. R_3, R_4, and R_5 differ because of different etch rates for various crystal faces. Under dilute conditions, the spontaneous polarization in this GaN layer leads to hole diffusion toward nitrogen face (right). (b) Schematic of bands for this structure when the top surface is exposed to an electrolyte.

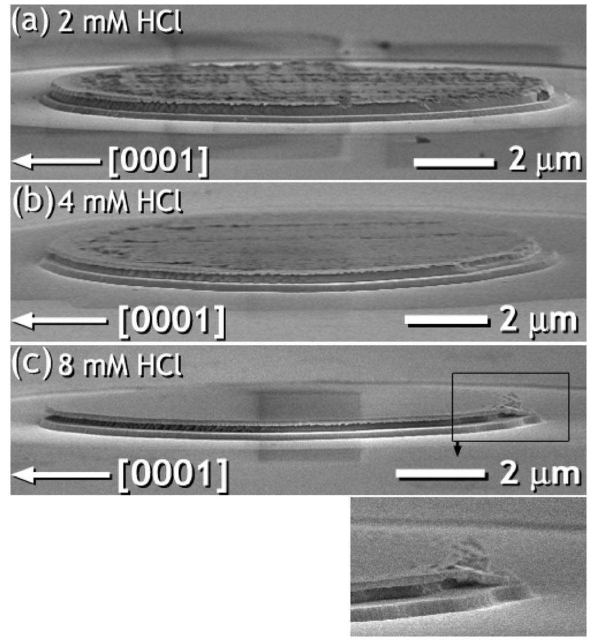

Figure 2. Passive microdisks etched using a 1000 W Xe lamp with a GaN filter in HCl of varying concentrations for 5 min: (a) 2, (b) 4, and (c) 8 mM HCl. In (a) and (b), the GaN disk layer is etched very significantly. In (c), only the right side (nitrogen face) of the GaN disk is etched, as shown in the zoomed-in image on the right.

layer, and these holes were consumed at different rates at all the surfaces of the material, indicated by R_1–R_5 in Fig. 1a. R_1 and R_2 are the lateral (undercut) etch rates of the $-c$ and $+c$ regions of the InGaN layer, R_3 and R_5 are the lateral etch rates of the $-c$ and $+c$ faces of the top GaN layer, and R_4 is the top-down etch rate of the *m*-plane GaN. Each of these rates was determined by the relative hole concentration, the crystallographic face, and the electrolyte concentration. In an ideal case, R_1 and R_2 would be equal and large, while R_3, R_4, and R_5 would be zero because holes would remain confined to the post region.

We first studied the effects of varying the HCl concentration during etching with a constant illumination intensity. Figure 2 shows three different microdisks, PEC etched in 2–8 mM HCl for 5 min. In all of these examples, the InGaN has formed an undercut, but the GaN disk layer has etched as well to varying degrees, meaning that the rates R_3, R_4, and R_5 are nonzero. When unilluminated, these structures do not etch at all, indicating that the source of the etching is indeed the photogenerated holes, which are only generated in the InGaN layer. Thus, some of the holes must drift into the GaN disk layer from the InGaN. The sample etched in the lowest HCl concentration had the least deep undercut, but the GaN disk on this sample was etched the most; i.e., the InGaN did not etch much, and the GaN, which should not etch at all, did etch significantly. In the sample etched in the highest HCl concentration, the undercut was the deepest, and there was the least damage to the GaN disk. If the etchant is strong, holes in the InGaN layer are consumed immediately in the etch process while they are still in the InGaN (i.e., R_1 and R_2 are much larger than R_3, R_4, and R_5). If the etchant is weak, the holes have time to drift into the GaN disk and be consumed there, leading to etching of this GaN layer (R_3, R_4, and R_5 become large).

In all the microdisks shown in Fig. 2 and in all the figures in this paper, the nitrogen-face ($-c$) side of the sample is on the right and the gallium-face ($+c$) side is on the left. In these microdisks, the N-face (right) side of the disk is where most of the unwanted etching occurs because holes are pushed to that side by the "in-plane" spontaneous polarization field indicated in Fig. 1a. In addition, many experiments have shown that the nitrogen face is more chemically reactive than the gallium face. These polarization fields and the crystallography are the reasons why rates R_3, R_4, and R_5 are different, and in some cases R_1 also differs from R_2. Because the nitrogen face is so much more reactive than the gallium face, $R_5 > R_4 > R_3$, as seen in Fig. 2.

For microdisk applications, we want the disk layers to remain completely intact and smooth. To accomplish this, we modified the epitaxial structure to prevent hole overflow into the disk. The simplest way to accomplish this is to increase the indium composition in the sacrificial layer, increasing the barrier height for holes to escape. In Fig. 3a, we show a disk with an $In_{0.05}Ga_{0.95}N$ sacrificial layer. This disk has its N-face (right) side etched; it also has some etch pits on the top. In Fig. 3b, there is a microdisk with an $In_{0.08}Ga_{0.92}N$ post, a higher indium composition. As grown, this sample was heavily pitted and looked black because of the high indium content of the 200 nm sacrificial layer. Although a microdisk with pits like these would not be an acceptable optical cavity, this experiment shows that increasing the indium content effectively reduces the damage to the disk layer caused by PEC etching: This sample looks symmetric with respect to the $+c$ and $-c$ directions, and there has been no etching of the GaN disk.

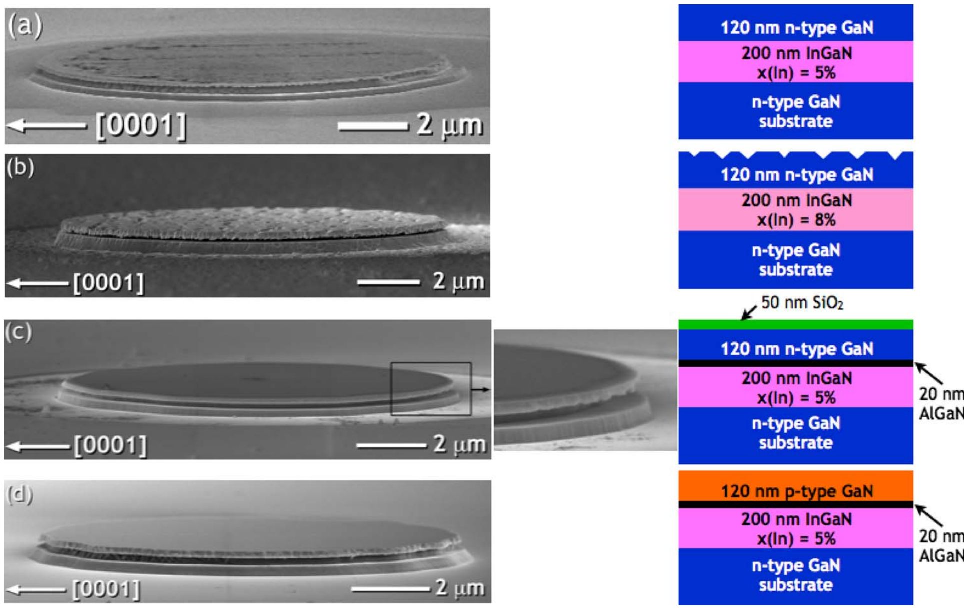

Figure 3. (Color online) Development of the epitaxial structure of the microdisk etched in 4 mM HCl with the Xe lamp and GaN filter for 5 min: SEM images of the completed devices are shown on the left, while schematics of the epitaxial designs used are shown on the right. None of these structures has quantum wells. (a) A disk with a low In composition post, (b) a disk with a high In composition post, (c) a structure similar to (b), but with a SiO_2 mask included during etching and AlGaN BL beneath the disk, and (d) a structure similar to (c), but without the SiO_2 mask and with the disk-doped p-type.

Another way to reduce hole overflow into the GaN disk is through the incorporation of an AlGaN blocking layer (BL). This technique has been successful in our *c*-plane microdisks: We are able to protect quantum wells in the disk from etching because the AlGaN blocks those electrons from being extracted, causing a recombination of electron–hole pairs in the quantum wells. As shown in Fig. 3c, we have used a lower indium composition but have added a 20 nm $Al_{0.12}Ga_{0.88}N$ layer to the bottom of the disk. Additionally, we left the SiO_2 hard mask on top of the sample during PEC etching, so that any holes that did diffuse into the GaN disk would not cause etching of the top GaN surface ($R_4 = 0$). This sample etched much more smoothly than the samples without an AlGaN BL, but there is still some unwanted etching visible from the roughness to the N-face underside of the disk, as shown in the boxed region. This indicates that AlGaN did not effectively block all the holes.

Finally, we doped the GaN disk layer p-type. Because of the surface band bending in p-type materials in contact with an electrolyte, p-type semiconductors are generally resistant to PEC etching.[13,14] Electrons are confined at the surface, and holes are pushed into the bulk. Selective undercut etching of p-n junctions has been reported because of the etch resistance of p-GaN.[13] As shown in Fig. 3d, the sample with a p-type doped disk was successfully undercut without any etching of the disk layer.

Next, we optimized the HCl concentration using the p-type disk structure to minimize crystallographic etching effects. Damage to the disk is no longer a problem with the p-type doping, but the quality of the undercut etch does vary with HCl concentration, as shown in Fig. 4. In this case, we varied the HCl concentration from 0.24 M (Fig. 4a) to 4 mM (Fig. 4e). Once again, the nitrogen face is on the right side of the image and the gallium face is on the left. In this case, holes are swept to the Ga-face side of the InGaN layers by the piezoelectric polarization in the strained layer and the Ga-face etches more rapidly than the N-face ($R_2 > R_1$). Crystallographic etch features are visible at higher concentrations (Fig. 4a-c). At lower concentrations (Fig. 4d and e) these crystallographic effects are less apparent, and the etch is predominantly photodriven in nature, providing a smooth and uniform undercut etch. Below 0.012 M HCl, the undercut is uniform for this lamp intensity.

Full microdisk structure.— For a fully functional microdisk, we need to incorporate a quantum well active region. The epitaxial structure shown in Fig. 5a was chosen for several reasons: (*i*) An AlGaN BL was included to suppress hole overflow into the disk. (*ii*) The multiple quantum well active region emits at 390 nm, higher in energy than the post, which emits at 410–420 nm, so that the sacrificial layer can be selectively excited during PEC etching. (*iii*) The p-type layer on top prevents etch pits from forming if holes overcome the AlGaN BL and enter the disk. (*iv*) The pin doping profile was chosen so that the microdisks could be electrically injected. For illumination, we used a high power (25 W) LED array with an emission wavelength of 405 nm, so that only the sacrificial layer was excited and not the quantum wells.

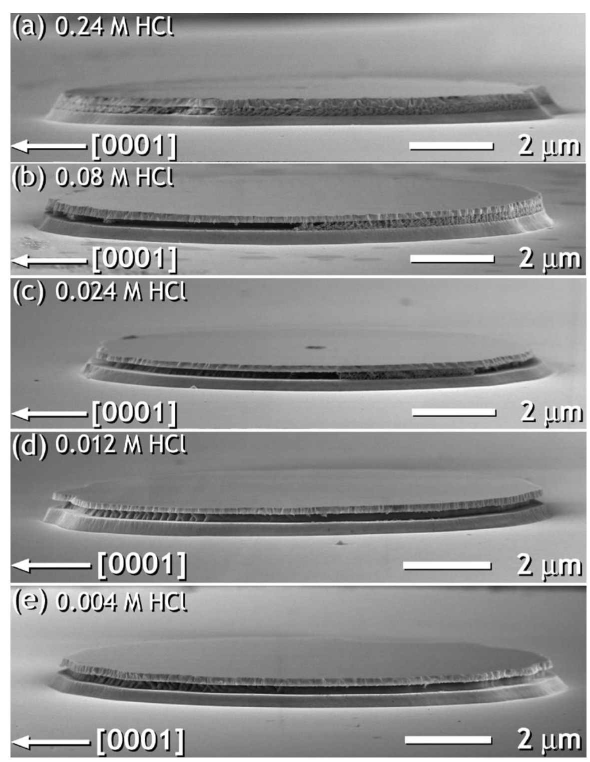

Figure 4. Using the p-type disk structure (Fig. 3d), we explored the HCl concentration dependence. The etches lasted for 5 min with illumination from the Xe lamp with a GaN filter (a) 0.24, (b) 0.08, (c) 0.024, (d) 0.012, and (e) 0.004 M HCl, at concentrations less than or equal to 0.012 M, $R_1 = R_2$.

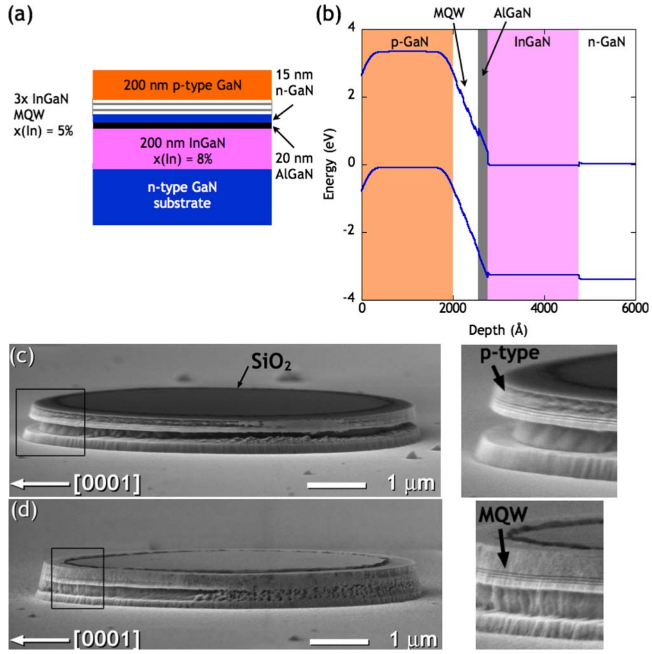

Figure 5. (Color online) A fully functional microdisk structure, including quantum wells and pin doping, etched using the LED lamp in 4 mM HCl for 15 min: (a) Epitaxial structure of these disks, (b) band diagram of this structure when in contact with an electrolyte, (c) a disk etched with the SiO_2 mask on, and (d) a disk with the SiO_2 mask removed before etching. A ring of residual SiO_2 remains.

As shown in Fig. 5c and d, there is still some etching of the disk, mainly in the quantum wells, but also in the cladding layers, including the p-GaN. Leaving the SiO_2 mask on during etching enhances the unwanted etch rates R_3 and R_5 (Fig. 5c). The band diagram indicates that excess holes can be easily swept into the p-GaN through the built-in electric field. Either the holes from the post are overcoming the AlGaN barrier (Fig. 5b) or there is some absorption of light by the quantum wells. Regardless of the cause, the solution is simple: Including a Ni/Au ohmic contact to the p-GaN during PEC etching causes the disk to be etch-resistant, as shown in Fig. 6. Because of the band bending introduced by the pin doping (Fig. 5b), holes are pushed into the p-type layer on top of the disk, where some may overcome the surface band bending to participate in etching reactions.[15] If a p-contact is included, however, holes are more likely to escape into the solution through the contact rather than through the bare p-GaN surface, where they can be extracted into the solution without causing an oxidation of the surface. Thus, holes in the post still lead to etching, while holes in the disk are extracted into the solution without causing unwanted etching.

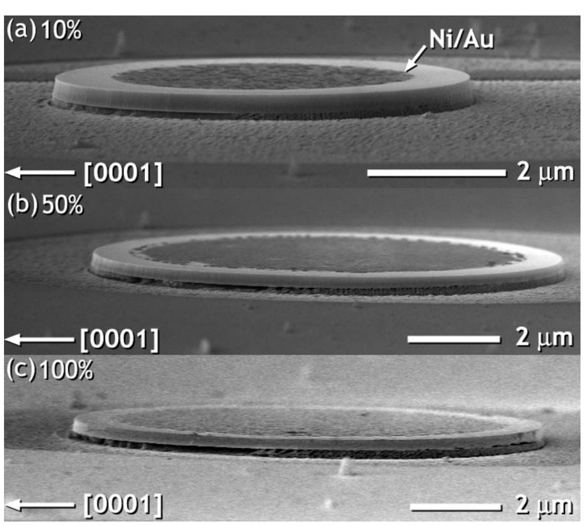

Figure 6. A study of LED lamp power dependence of undercut etching in 4 mM HCl for 15 min: These microdisks all have a Ni/Au p-contact to prevent etching of the p-GaN disk. (a) 10, (b) 50, and (c) 100% LED power. In all cases, the disk layer has not etched, but the extent and symmetry of the undercut depend strongly on incident illumination intensity, with the best results (c) at the highest lamp power.

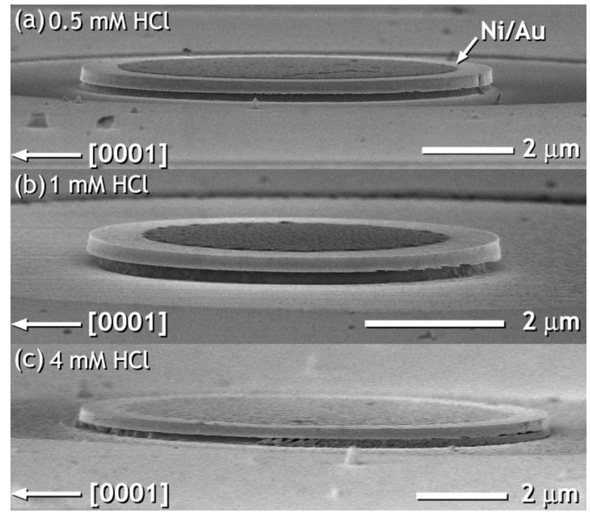

Figure 7. Microdisks etched with the LED lamp at 100% power, but with varying HCl concentration: (a) 0.5 mM HCl, 30 min etch; (b) 1 mM HCl, 30 min etch; and (c) 4 mM HCl, 15 min etch. At concentrations less than or equal to 1 mM, $R_1 = R_2$, and the undercut is symmetric.

Because we switched to using a lamp for PEC etching, it was necessary to calibrate both the lamp power and the HCl concentration for optimal etch results. Microdisks etched under LED lamp powers from 10 to 100% are shown in Fig. 6. In all of these etches, the electrolyte was 4 mM HCl. The degree of undercut varies with lamp power, and the maximum lamp power yields the best results, although there are still some crystallographic effects visible in the undercut in Fig. 6c. Decreasing the HCl concentration, as we did with the Xe lamp, helps eliminate these crystallographic effects, as shown in Fig. 7. No crystallographic etching is observed below 1 mM HCl at full lamp power. Under these conditions, the disk is intact and smoothly undercut. However, the reduced power of the LED lamp compared to that of the Xe lamp means that the ideal HCl concentration and thus the etch rate are lower. For these lower concentrations, we increased the etch time from 15 to 30 min. Using this fabrication procedure, we made 6 μm diameter *m*-plane microdisks. A completed device is shown in Fig. 8, and the Ni/Au p-contact is visible in this SEM image. This disk was etched in 1 mM HCl, 100% lamp power for 1 h. The undercut and optical cavity

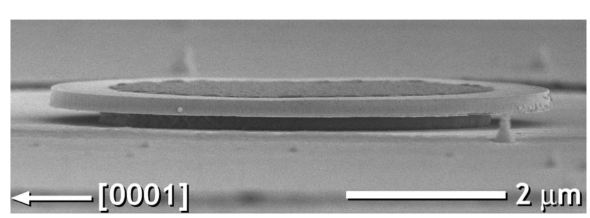

Figure 8. An SEM image of a 6 μm *m*-plane microdisk. This disk was etched in 1 mM HCl, 100% LED lamp power for 1 h with a Ni/Au p-contact.

are much smoother than in our previous *c*-plane microdisks.[7] We reported on the optical and electrical properties of these microdisks elsewhere.[16]

Conclusions

In summary, we have explored bandgap-selective PEC etching of *m*-plane GaN for undercut etching applications. We have studied the dependence of undercut quality on etchant concentration, illumination intensity, masking material, and epitaxial structure. In these nonpolar microdisks, the in-plane polarization fields have a dramatic effect on the symmetry of the etching in both the undercut etching and in the unwanted etching of the GaN disk layer. With a careful balance of etchant concentration and illumination intensity and a well-designed epitaxial structure, it is possible to achieve undercut etching that leads to smoother optical cavities than we could achieve with *c*-plane GaN. Using this technique, we have successfully fabricated *m*-plane microdisks. The detailed electrical and optical performance of these microdisks are reported elsewhere.[16]

Acknowledgments

A.C.T. is supported by the Department of Defense National Defense Science and Engineering Graduate Fellowship. Research funding was provided by the Solid State Lighting and Energy Center. This work made use of the University of California, Santa Barbara nanofabrication facility, part of the National Science Foundation-funded National Nanotechnology Infrastructure Network.

University of California assisted in meeting the publication costs of this article.

References

1. N. Akopian, G. Bahir, D. Gershoni, M. D. Craven, J. S. Speck, and S. P. DenBaars, *Appl. Phys. Lett.*, **86**, 202104 (2005).
2. S. F. Chichibu, A. Uedono, T. Onuma, B. A. Haskell, A. Chakraborty, T. Koyama, Paul. T. Fini, S. Keller, S. P. DenBaars, et al., *Nature Mater.*, **5**, 810 (2006).
3. A. C. Tamboli, M. C. Schmidt, S. Rajan, J. S. Speck, U. K. Mishra, S. P. DenBaars, and E. L. Hu, *J. Electrochem. Soc.*, **156**, H47 (2009).
4. C. Meier, K. Hennessy, E. D. Haberer, R. Sharma, Y. S. Choi, K. McGroddy, S. Keller, S. P. DenBaars, S. Nakamura, and E. L. Hu, *Appl. Phys. Lett.*, **88**, 031111 (2006).
5. B. Yang and P. Fay, *J. Vac. Sci. Technol. B*, **24**, 1337 (2006).
6. R. Sharma, E. D. Haberer, C. Meier, E. L. Hu, and S. Nakamura, *Appl. Phys. Lett.*, **91**, 211108 (2007).
7. A. C. Tamboli, E. D. Haberer, R. Sharma, K. H. Lee, S. Nakamura, and E. L. Hu, *Nat. Photonics*, **1**, 61 (2007).
8. D. Zhuang and J. H. Edgar, *Mater. Sci. Eng. R.*, **48**, 1 (2005).
9. E. D. Haberer, R. Sharma, A. R. Stonas, S. Nakamura, S. P. DenBaars, and E. L. Hu, *Appl. Phys. Lett.*, **85**, 762 (2004).
10. Y. Gao, I. Ben-Yaacov, U. K. Mishra, and E. L. Hu, *J. Appl. Phys.*, **96**, 6925 (2004).
11. C.-F. Lin, Z.-J. Yang, B.-H. Chin, J.-H. Zheng, J.-J. Dai, B.-C. Shieh, and C.-C. Chang, *J. Electrochem. Soc.*, **153**, G1020 (2006).
12. M. S. Minsky, M. White, and E. L. Hu, *Appl. Phys. Lett.*, **68**, 1531 (1996).
13. C. Youtsey, G. Bulman, and I. Adesida, *J. Electron. Mater.*, **27**, 282 (1998).
14. R. Khare and E. L. Hu, *J. Electrochem. Soc.*, **138**, 1516 (1991).
15. A. C. Tamboli, A. Hirai, S. Nakamura, S. P. DenBaars, and E. L. Hu, *Appl. Phys. Lett.*, **94**, 151113 (2009).
16. A. C. Tamboli, M. C. Schmidt, A. Hirai, S. P. DenBaars, and E. L. Hu, *Appl. Phys. Lett.*, **94**, 251116 (2009).